LITHIUM, SODIUM, AND POTASSIUM RESONANCE LINES PRESSURE BROADENED BY HELIUM ATOMS

Robert Beuc[1], Gillian Peach[2], Mladen Movre[1], and Berislav Horvatić[1]
[1] Institute of Physics, HR-10000 Zagreb, Croatia
[2] University College London, London WC1E 6BT, UK

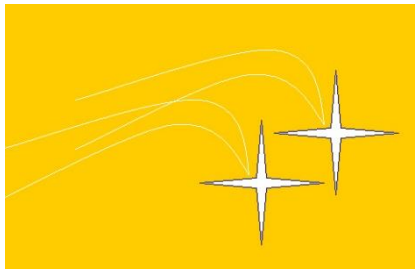

X Serbian - Bulgarian Astronomical Conference

Introduction

- In the last two decades the pressure broadening of alkali-metal resonance lines has gained a new importance in astrophysical research as well. It has been found that prominent features in the spectra of brown dwarfs and extrasolar giant planets might be attributed to the resonance lines of the alkali-metal atoms broadened by collisions with the ambient hydrogen molecules and helium atoms (Burrows et al. 2003; Sharp et al. 2007).
- Detailed knowledge of the line profiles as functions of temperature and pressure enable the interpretations of the observed spectra, which yield information on the temperatures, densities, albedos and compositions of the stellar atmospheres.
- We carried out calculations of the emission and absorption spectra in the far wings of the first resonant doublets of light alkalies for temperatures from 500 to 3000 K.

Potential curves and transition dipole moments of alkali-helium dimers

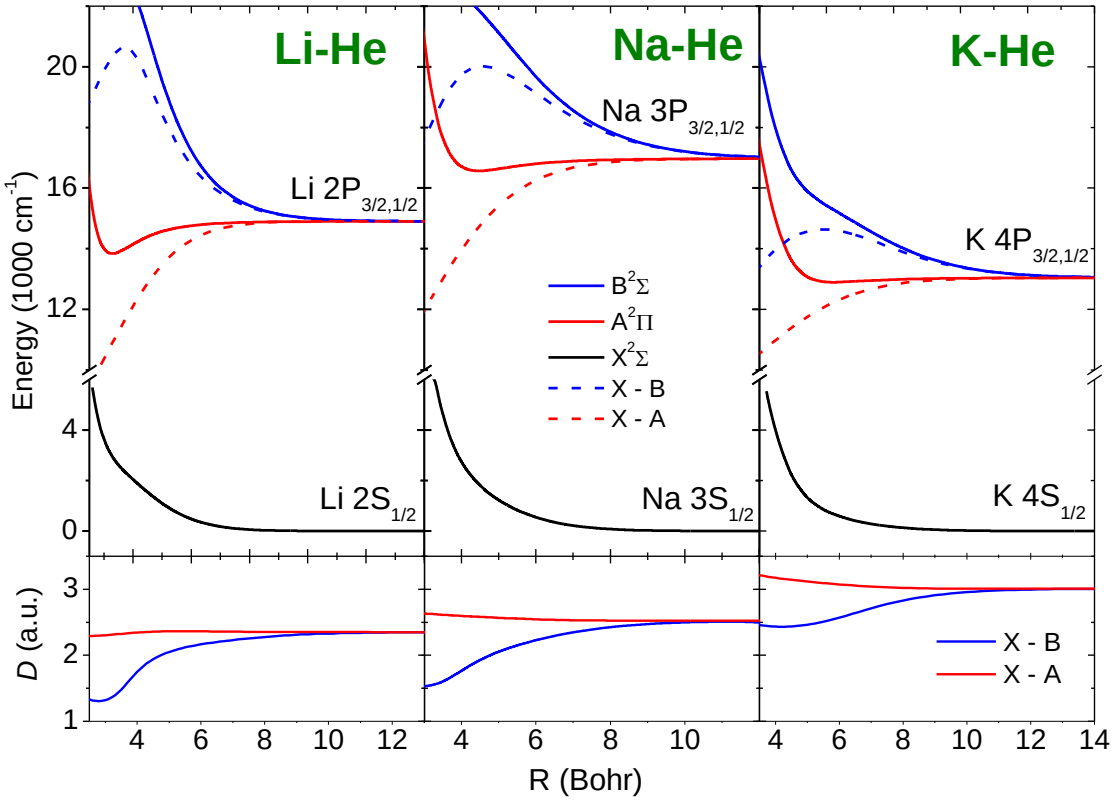

Molecular-structure calculations of A-He molecules have been performed neglecting the spin-orbit interaction. The A-He molecule is treated in a three-body model, as an A^+ ion plus a valence electron and a He atom, represented by a polarizable atomic core (Peach 1982; Mullamphy et al. 2007). The electron helium atom and electron alkali ion interactions are represented by model potentials.

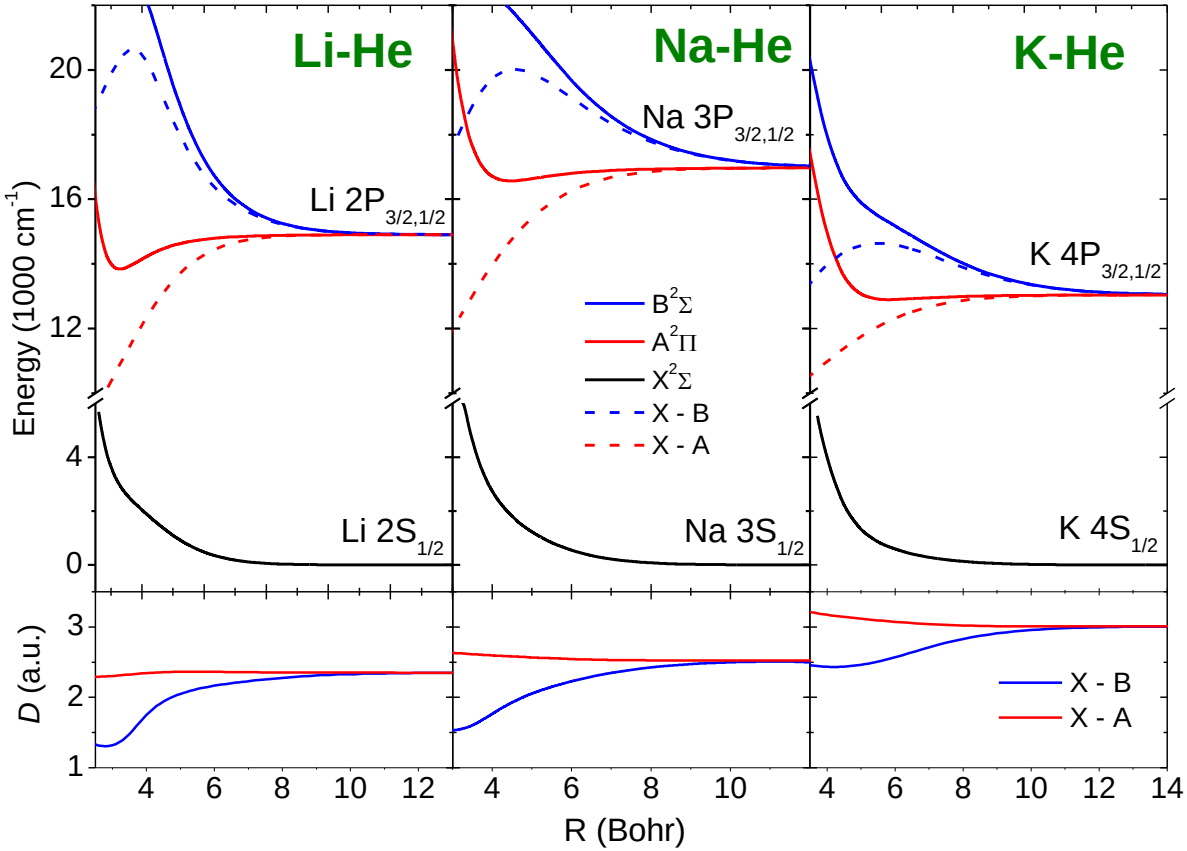

Potential curves, difference potential curves (dashed lines) and transition dipole moments *D(R)* (second row) of the lowest electronic states have qualitatively the same shape for all three dimers.

- The ground **$X^2\Sigma^+$** and the excited **$B^2\Sigma^+$** state potential curves are predominantly repulsive, exhibiting just a shallow well at large interatomic distances.
- The excited **$A^2\Pi$** states have the potential well at small interatomic distances (R_e = 3.3 a_0, D_e = 1060.2 cm^{-1}), (R_e = 4.4 a_0, D_e = 422.8 cm^{-1}), and (R_e = 6.2 a_0, D_e = 129.2 cm^{-1}).
- ***X-A*** transition has a monotonic difference potential curve and contributes to the "red" wing of the first resonant line.
- ***X-B*** transition has a difference potential curve with one maximum and contribute to the "blue" wing and "blue" satellite band.

Quantum calculation on the Fourier grid

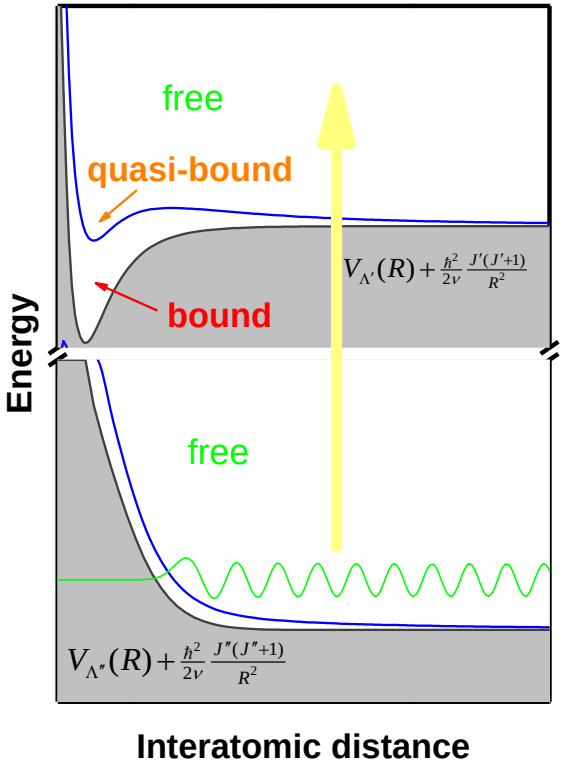

The thermally averaged absorption coefficient comprises contributions from the transitions between all the rovibrational states of a lower Λ" and the upper Λ′ electronic state. In each electronic state there is a finite number of bound and quasi-bound states with unity-normalized wave functions $\Phi_{v,J,\Lambda}(R)$ (v vibrational, J rotational quantum number), and an infinite continuum of free rovibrational states with energy-normalized wave functions $\Phi_{\varepsilon,J,\Lambda}(R)$.

Quantum calculation on the Fourier grid

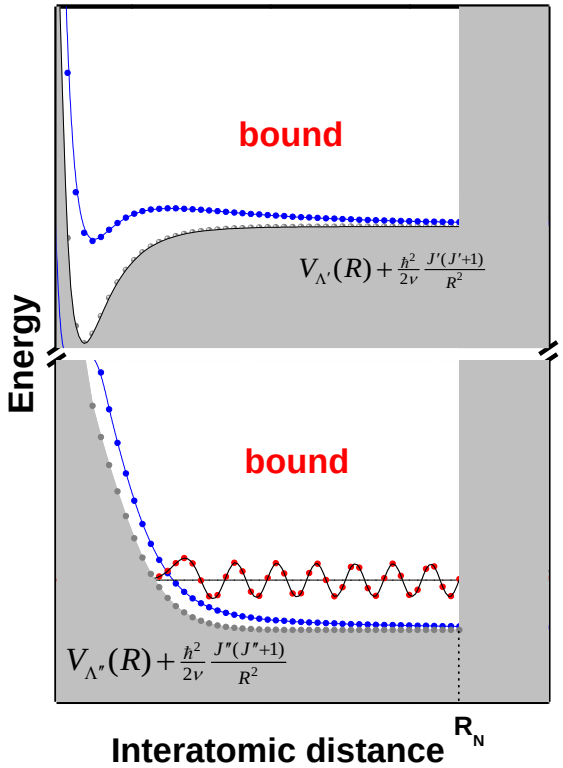

In the Fourier grid Hamiltonian method (FGH), rovibrational wave functions are represented on a finite number of uniformly spaced grid points R_i (i=1,…N), $\Phi_{v(\varepsilon),J,\Lambda}(R) \rightarrow \Phi_{v(\varepsilon),J,\Lambda}(R_i)$. The Hamiltonian is represented on the grid by an NxN matrix:

$$H(\Lambda,J)_{i,j}=\begin{cases} V_\Lambda(R_i)+\frac{\hbar^2}{2\mu}\frac{J(J+1)+\Lambda^2}{R_i^{\,2}}+\frac{\hbar^2}{2\mu\Delta R^2}\frac{2\pi^2 i^2-3}{6i^2} & i=j \\ \frac{\hbar^2}{2\mu\Delta R^2}\frac{8ij(-1)^{i-j}}{\left(i^2-j^2\right)^2} & i\neq j \end{cases}$$

$V_\Lambda(R)$ is the adiabatic potential of the electronic state, Λ the electronic angular moment of this state, ΔR the distance between neighbouring grid points, and μ the reduced mass of the molecule.

The *infinite* set of rovibrational states is represented on the grid by a *finite* set of states whose energies $E_{v,J,\Lambda}$ and wave functions $\Phi_{v,J,\Lambda}$ (v=1,….N) are eigenvalues and eigenvectors of the Hamiltonian matrix ***H(Λ,J)***. The *continuum* of free states is represented by a *discrete* set of unity-normalized wave functions having a node at outer grid boundary $R_N = N\,\Delta R$.

In LTE and binary (low-pressure) approximation, assuming the Q-branch approximation (*ΔJ=0*), the **reduced absorption coefficient** **(RAC)** for temperature *T* and frequency *v* has the form (Beuc et al. 2012; Chung et al. 2001):

$$k(\nu,T) = w\frac{h^2\nu}{c}\left(\frac{2\pi}{\mu k_B T}\right)^{3/2}\sum_{J}^{J_{\max}}(2J+1)\sum_{\mathrm{v}'',\mathrm{v}'}^{\mathrm{N,N}}\exp\left(-\frac{E_{\mathrm{v}'',J,\Lambda''}}{k_B T}\right)\left|\left\langle\Phi_{\mathrm{v}'',J,\Lambda''}\left|D(R)\right|\Phi_{\mathrm{v}',J,\Lambda'}\right\rangle\right|^2 g(\nu-\nu_{tr})$$

w is a statistical factor (1/3 *for X-B*, 2/3 for *X-A* transitions), $J_{\max}$ is the largest J value, *g*(*v*) is the instrumental profile, and transition frequencies are $\nu_{tr} = (E_{\mathrm{v}',J,\Lambda'} - E_{\mathrm{v}'',J,\Lambda''})/h$

The parameters for the calculation are estimated in the following way.:

- We chose the local radial kinetic energy cut-off at $E_N = 5k_BT_{max}$.
- The step size is given by $\Delta R = \pi\hbar\sqrt{2\mu E_N}$.
- J_{max} was estimated according to $\frac{\hbar^2 J_{max}^2}{2\mu R_J^2} \cong E_N$, where $R_J \leq R_N$, $V_\Lambda(R_J) \approx V_\Lambda(\infty)$.

  We chose R_J = 13, 14, 15 a_0 and get J_{max} = 288, 333, 343 for Li-, Na-, K-He, respectively.
- We chose N =500 grid points and get R_N = 76, 66, 64 a_0.

In LTE and binary (low-pressure) approximation, assuming the Q-branch approximation (*ΔJ=0*), the **reduced absorption coefficient (RAC)** for temperature *T* and frequency *ν* has the form (Beuc et al. 2012; Chung et al. 2001):

$$k(\nu,T) = w\frac{h^2\nu}{c}\left(\frac{2\pi}{\mu k_B T}\right)^{3/2}\sum_{J}^{J_{\max}}(2J+1)\sum_{\mathrm{v}'',\mathrm{v}'}^{\mathrm{N,N}}\exp\left(-\frac{E_{\mathrm{v}'',J,\Lambda''}}{k_B T}\right)\left|\left\langle\Phi_{\mathrm{v}'',J,\Lambda''}\left|D(R)\right|\Phi_{\mathrm{v}',J,\Lambda'}\right\rangle\right|^2 g(\nu-\nu_{tr})$$

w is a statistical factor (1/3 *for X-B*, 2/3 for *X-A* transitions), $J_{\max}$ is the largest J value, *g*(*ν*) is the instrumental profile, and transition frequencies are $\nu_{tr} = (E_{\mathrm{v}',J,\Lambda'} - E_{\mathrm{v}'',J,\Lambda''})/h$

We used about 5-6 min of the computer time to calculate all the necessary matrix elements for each molecule. To evaluate the absorption coefficient for a given temperature, spectrum is collected in bins of the size $\Delta\nu/c$ = 2 cm^{-1}, and smoothed with a triangle profile (FWHM 10 cm^{-1}) consuming 20-25 seconds of computer time.

In the neighbourhood of the atomic line transition frequencie ν_0, for an optically thick medium, the **emission coefficient (EC)** is simply related to (RAC) (Horvatić et al. 2015)

$$\varepsilon(\nu,T) = \frac{8\pi\nu^2}{c^2}e^{-\frac{h(\nu-\nu_0)}{k_B T}}k(\nu,T)$$

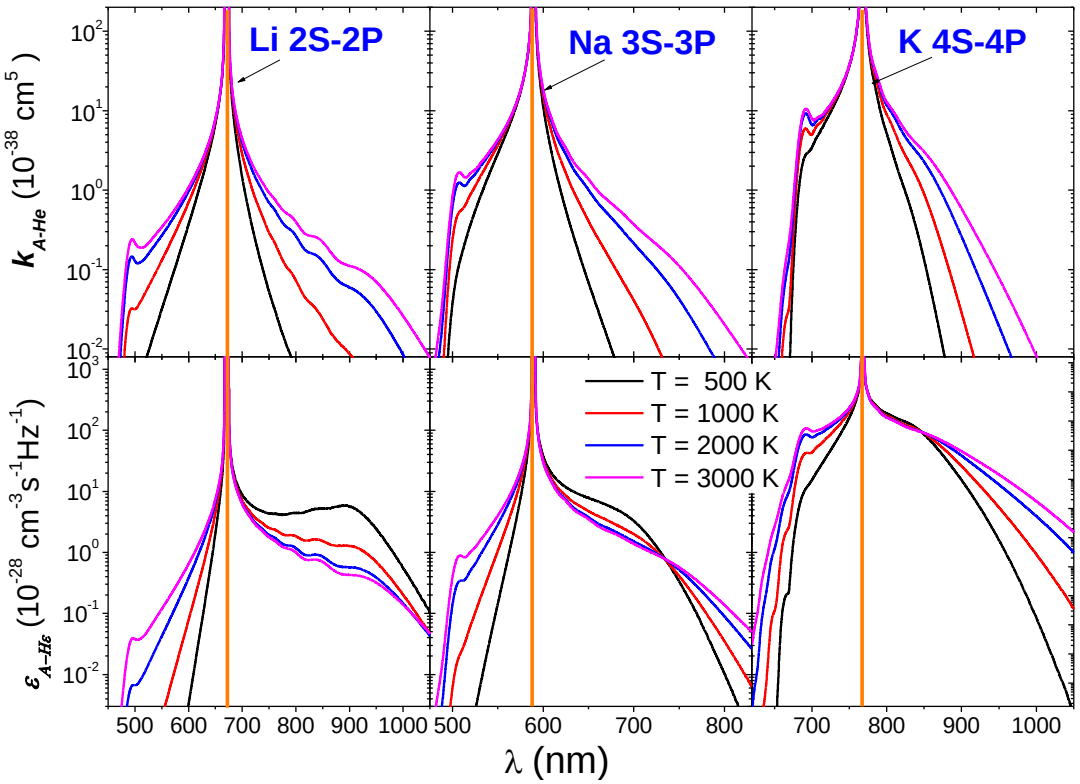

Reduced absorption coefficient (RAC)

Emission coefficient (EC)

- RAC and EC of A-He dimers exhibit the same qualitative behaviour.
- RAC increase with temperature because the initial $\mathbf{X^2\Sigma^+}$ state is repulsive.
- EC in the blue wing (*X-B* transition) increases with temperature because of the repulsive initial state $\mathbf{B^2\Sigma^+}$. The wing terminates with a blue satellite band as a consequence of an extremum in the *X-B* transition difference potential curve.

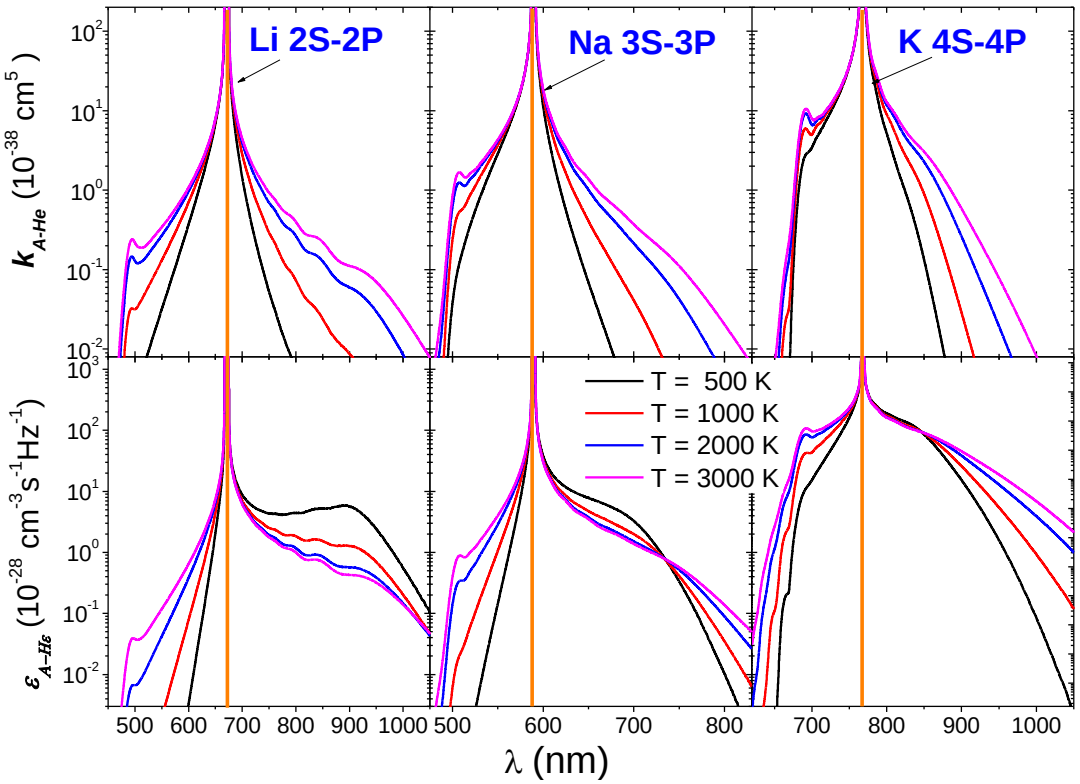

Reduced absorption coefficient (RAC)

Emission coefficient (EC)

- In the red wing where Condon transitions are connected with the attractive well of **$A^2\Pi$** state, Stückelberg oscillations occur. These oscillations increase with temperature and the potential well depth in **$A^2\Pi$** states.
- The red wing EC increases with temperature in the spectral range where Condon transitions are connected with a repulsive part of **$A^2\Pi$** , and decreases in the region where Condon transitions are connected with attractive part of this state. As a consequence, there is a broad plateau in the red wing at low temperatures.

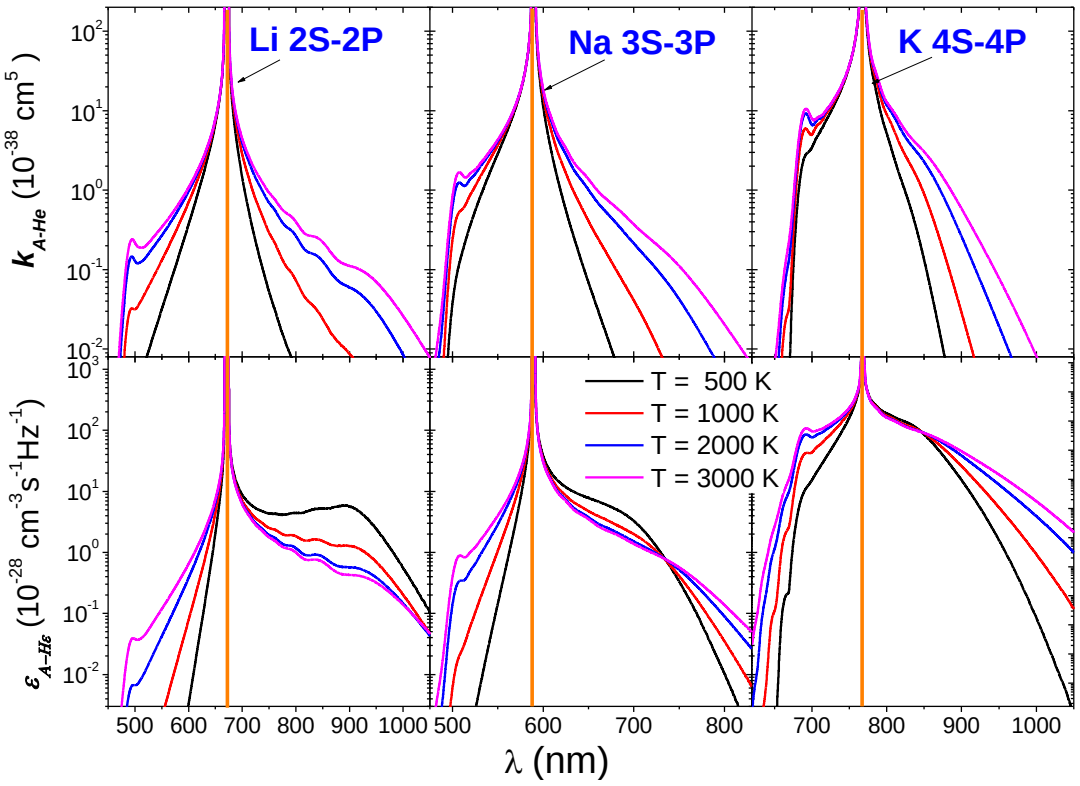

Our calculations are in good agreement with previous theoretical and experimental results. There is a small difference in satellite positions and intensities due to the difference in molecular potential curves applied.

Li-He blue satellite 497 nm, Lalos et al. (1962) 530, Zhu et al. (2005) 536, Allard et al. (2014) 526, 500 nm

red-wing emission plateau at 892 nm, Scheps et al. (1975) 900, Zhu et al. (2005) 870 nm.

Na-He blue satellite 508nm, Chung et al. (2002) 530, Zhu et al. (2006) 532, Alioua et al. (2008) 528 nm.

K-He blue satellite 692.5nm, Zhu et al. (2006) 708, Baab et al. (2010) 710 nm

Using the potential data of Schmidt-Mink et al. (1985) for Li_2, Magnier (1993) for Na_2 and Yan & Meyer for K_2 molecule, we calculated RAC of A_2 dimers, which decrease with temperature and are much larger than A-He RAC because of the deep well of the A_2 ground-state potential.

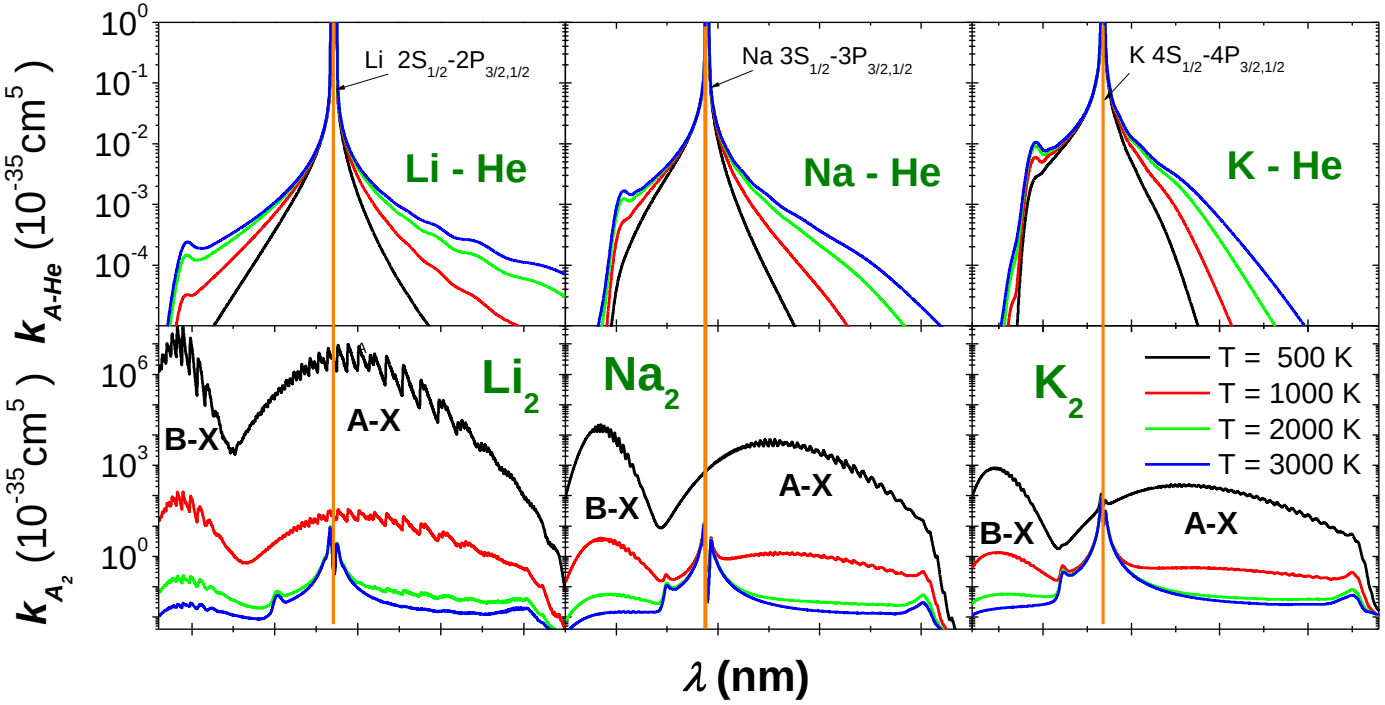

The optical depth of a uniform layer of thickness L, alkali number density N_A, helium number density N_{He}:

$$\tau(T,\nu) = LN_{He}N_A k_{A-He}(T,\nu) + LN_A^2 k_{A_2}(T,\nu)$$

To observe the broadening of alkali lines by He, the partial optical depth of A-He must be comparable to or larger then the partial depth of A_2. This holds for higher temperatures and/or if the abundance of helium is much larger then alkali, which is satisfied in a stellar atmosphere.

Conclusions

In order to get a powerful tool for analyzing the atmospheres of brown dwarfs, one needs:

- precise molecular potential curves and transition dipole moments,
- a correct and time-efficient spectral simulation (we believe that our FGH method is one of such),
- and laboratory experimental verification in a large interval of temperatures and pressures. The last requirement is probably the hardest one to achieve.